

Optimal electromagnetic energy transmission and real-time dissipation in extended media

S. Glasgow¹ and M. Ware^{2,*}

¹*Department of Mathematics, Brigham Young University, Provo, Utah 84602, USA*

²*Department of Physics and Astronomy, Brigham Young University, Provo, Utah 84602, USA*

[*ware@byu.edu](mailto:ware@byu.edu)

Abstract: Pulse reshaping effects that give rise to fast and slow light phenomena are inextricably linked to the dynamics of energy exchange between the pulse and the propagation medium. Energy that is dissipated from the pulse can no longer participate in this exchange process, but previous methods of calculating real-time dissipation are not valid for extended propagation media. We present a method for calculating real-time dissipation that is valid for electromagnetic pulse propagation in extended media. This method allows one to divide the energy stored in an extended medium into the portion that can be later transmitted out of the medium, and that portion which must be lost to either dissipation or reflection.

© 2014 Optical Society of America

OCIS codes: (350.5500) Propagation; (260.2110) Electromagnetic theory; (260.2030) Dispersion.

References and links

1. L. V. Hau, S. E. Harris, Z. Dutton, and C. H. Behroozi, "Light speed reduction to 17 metres per second in an ultracold atomic gas," *Nature* **397**, 594–598 (1999).
2. M. M. Kash, V. A. Sautenkov, A. S. Zibrov, L. Hollberg, G. R. Welch, M. D. Lukin, Y. Rostovtsev, E. S. Fry, and M. O. Scully, "Ultraslow group velocity and enhanced nonlinear optical effects in a coherently driven hot atomic gas," *Phys. Rev. Lett.* **82**, 5229–5232 (1999).
3. S. Inouye, R. F. Löw, S. Gupta, T. Pfau, A. Görlitz, T. L. Gustavson, D. E. Pritchard, and W. Ketterle, "Amplification of light and atoms in a bose-einstein condensate," *Phys. Rev. Lett.* **85**, 4225–4228 (2000).
4. S.-W. Chang, S.-L. Chuang, P.-C. Ku, C. J. Chang-Hasnain, P. Palinginis, and H. Wang, "Slow light using excitonic population oscillation," *Phys. Rev. B* **70**, 235333 (2004).
5. J. Sharping, Y. Okawachi, and A. Gaeta, "Wide bandwidth slow light using a raman fiber amplifier," *Opt. Express* **13**, 6092–6098 (2005).
6. R. Camacho, M. Pack, J. Howell, and R. Boyd, "Wide-bandwidth, tunable, multiple-pulse-width optical delays using slow light in cesium vapor," *Phys. Rev. Lett.* **98**, 153601 (2007).
7. R. W. Boyd, "Slow and fast light: fundamentals and applications," *J. Mod. Opt.* **56**, 1908–1915 (2009).
8. Z. Shi, R. W. Boyd, D. J. Gauthier, and C. C. Dudley, "Enhancing the spectral sensitivity of interferometers using slow-light media," *Opt. Lett.* **32**, 915–917 (2007).
9. F. Xia, L. Skaric, and Y. Vlasov, "Ultracompact optical buffers on a silicon chip," *Nat. Photonics* **1**, 65–71 (2007).
10. M. Ware, S. Glasgow, and J. Peatross, "Role of group velocity in tracking field energy in linear dielectrics," *Opt. Express* **9**, 506–518 (2001).
11. V. S. Zapasskii and G. G. Kozlov, "A saturable absorber, coherent population oscillations, and slow light," *Opt. Spectrosc.* **100**, 419–424 (2006).
12. M. Ware, S. Glasgow, and J. Peatross, "Energy transport in linear dielectrics," *Opt. Express* **9**, 519–532 (2001).
13. S. Glasgow, M. Meilstrup, J. Peatross, and M. Ware, "Real-time recoverable and irrecoverable energy in dispersive-dissipative dielectrics," *Phys. Rev. E* **75**, 016616 (2007).
14. S. A. Glasgow and M. Ware, "Real-time dissipation of optical pulses in passive dielectrics," *Phys. Rev. A* **80**, 043817 (2009).

15. G. Gentili, "Free enthalpies, free energies and norms for dielectrics with fading memory," *Continuum Mech. Thermodyn.* **8**, 201–214 (1996).
 16. V. Berti and G. Gentili, "The minimum free energy for isothermal dielectrics with memory," *J. Non-Equilib. Thermodyn.* **24**, 154–176 (1999).
 17. M. Fabrizio and A. Morro, "Dissipativity and irreversibility of electromagnetic systems," *Math. Models Methods Appl. Sci.* **10**, 217–246 (2000).
 18. L. Deseri, G. Gentili, and M. Golden, "An explicit formula for the minimum free energy in linear viscoelasticity," *J. Elasticity* **54**, 141–185 (1999).
 19. J. M. Golden, "Consequences of non-uniqueness in the free energy of materials with memory," *Int. J. Eng. Sci.* **39**, 53–70 (2001).
 20. J. M. Golden, "A proposal concerning the physical rate of dissipation in materials with memory," *Q. Appl. Math.* **63**, 117–155 (2005).
-

1. Introduction

Slow light can be achieved in a variety of physical systems [1–6] where the group velocity for the medium can be made much smaller than c over a certain spectral range. Such phenomena have shown promise for interferometry [7,8] and other applications such as telecommunications where an all-optical method for pulse delay would be helpful [9]. The slow light phenomenon is most frequently analyzed using frequency techniques [10], but time-domain analysis can also yield insights into the physical processes that give rise to slow propagations [11, 12].

In time-domain analysis of slow light pulses, slow light phenomena are thought of in terms of pulse reshaping. The early portions of the pulse transfer energy into the propagation medium while later portions recover a portion of this energy back from the propagation medium to the pulse [12]. The combined effect of this energy transfer shifts the pulse arrival times to later times, and the peak of the pulse is observed to propagate at "slow" speeds.

This energy transfer process is not perfectly efficient, and energy dissipates from electromagnetic fields to thermal energy as a pulse interacts with the propagation medium. Dissipated energy cannot be returned to the latter portions of the pulse, so understanding the timing of when energy shifts from the "undissipated" to the "dissipated" status can help one understand the slow-light propagation process. In this article we introduce a framework for describing the real-time dynamics of energy dissipation as a pulse interacts with an extended propagation medium.

We previously detailed an approach for calculating real-time loss that was appropriate for point-wise analysis [13, 14]. This previous analysis was analogous to other methods developed to describe dissipation in general viscoelastic and dielectric media [15–20]. However, each of these methods of analysis calculates the energy density at single point within the medium (or, in the case of viscoelasticity, treats physically extended elements "en masse," hence as point-like). This point-wise analysis can lead to incorrect results when analyzing the propagation of an energy pulse through a distributed medium.

To understand why the transition from a point-wise energy density approach to analyzing a distributed medium causes troubles, we briefly review the two previous methods we use to analyze dissipation. The first method [13] divides the energy stored in a dielectric in two forms: recoverable and irrecoverable energy. The recoverable energy density at any given time is the fraction of energy that could possibly be transferred from the medium back to the field by an appropriately chosen future field. The remaining irrecoverable energy density $u_{\text{irrec}}(t)$ cannot be retrieved from the medium regardless of what happens in the future, and thus gives an upper bound for the dissipation up to time t .

The second method for analyzing real-time dissipation [14] identifies the past field that could have created the pulse-medium state with the least amount of energy being deposited in the medium. The difference between the actual amount of energy deposited in the medium and the minimum value required to create the current pulse-medium excitation gives $u_{\text{waste}}(t)$, the

amount of energy density that has been “wasted” in creating the pulse-medium state at a given point in time. Since $u_{\text{waste}}(t)$ represents the minimum amount of energy that must have been dissipated up to a given time, it gives the lower bound for energy dissipation up to time t .

The combination of $u_{\text{waste}}(t)$ and $u_{\text{irrec}}(t)$ define a range of acceptable values for the real-time dissipation up to time t at a given point. This range is a natural reflection of the fact that the transformation to random thermal energy does not happen at a precise instant, so the amount of dissipation as a function of time is necessarily “fuzzy.” However, any point-wise notion of real-time loss that is smaller than the waste energy density or larger than the irrecoverable energy cannot be associated with a (macroscopically) possible process of energy flow.

When fields propagate through an extended medium, the electric field changes slightly at each successive point due its interaction with previous points. This makes the point-wise analysis of energy dissipation inappropriate for propagation problems where energy is distributed throughout a medium. For example, it may be tempting to calculate $u_{\text{irrec}}(z, t)$ at each point in the medium and then integrate over space to find the total irrecoverable energy. This approach is incorrect since it calculates optimum future fields for each point *independent of all other points in the medium*. These independently chosen future fields are typically incompatible because they do not satisfy the causal connections required by Maxwell’s equations between points in the medium. Calculating the real-time dissipation using this naive approach would underestimate the amount of dissipation that has occurred up to a given time.

In this paper, we present methods for describing real-time dissipation for pulse propagation in an extended medium one-dimensional medium. This method considers fixed past fields and potential future fields that are consistent (via Maxwell’s equations) throughout the medium. This method treats the loss in the medium as a whole, rather than focusing on a single point, so that the results can be used to analyze propagation appropriately. The approach in this paper is analogous to the first point-wise method which yields u_{irrec} .

2. Definitions

We consider a one-dimensional dielectric slab located in a region $0 \leq z \leq L$ with vacuum on either side, and linearly polarized “planar” pulses of the form

$$\begin{aligned}\mathbf{E}(z, t) &= E(z, t)\mathbf{j}, \\ \mathbf{P}(z, t) &= P(z, t)\mathbf{j}, \\ \mathbf{H}(z, t) &= H(z, t)\mathbf{i}\end{aligned}\tag{1}$$

propagating in the \mathbf{k} direction through this system, where \mathbf{i} , \mathbf{j} , and \mathbf{k} are the typical unit vectors along x , y , and z . For a linear isotropic medium, the dielectric polarization field \mathbf{P} is related to \mathbf{E} through the susceptibility $\chi(\omega)$ via

$$\hat{P}(z, \omega) = \chi(\omega) (\theta^+(z) - \theta^+(z-L)) \hat{E}(z, \omega),\tag{2}$$

where θ^+ denotes the unit step supported only for positive argument. The “hat” notation indicates the Fourier transform of a temporal field, defined by

$$\begin{aligned}\hat{F}(z, \omega) &= \frac{1}{\sqrt{2\pi}} \int_{-\infty}^{+\infty} dt F(z, t) e^{+i\omega t} \\ F(z, t) &= \frac{1}{\sqrt{2\pi}} \int_{-\infty}^{+\infty} d\omega \hat{F}(z, \omega) e^{-i\omega t}.\end{aligned}\tag{3}$$

The pulse described by Eq. (1) must satisfy Maxwell's equations, which, for our geometry, are given by

$$\hat{H}(z, \omega) = \frac{c}{-i\omega} \hat{E}'(z, \omega) \quad (4)$$

and

$$\hat{E}''(z, \omega) = -\frac{\omega^2}{c^2} (1 + \chi(\omega) [\theta^+(z) - \theta^+(z-L)]) \hat{E}(z, \omega) \quad (5)$$

in the frequency domain. For a pulse originating from $z = -\infty$ and impinging on the interface located at $z = 0$, we can write the electric field solution to Maxwell's equations in the form

$$\hat{E}(z, \omega) = \begin{cases} \hat{E}_i(\omega) e^{ik_0(\omega)z} + \hat{E}_r(\omega) e^{-ik_0(\omega)z} & z \leq 0 \\ \hat{E}_f(\omega) e^{ik(\omega)z} + \hat{E}_b(\omega) e^{-ik(\omega)z} & 0 \leq z \leq L \\ \hat{E}_t(\omega) e^{ik_0(\omega)(z-L)} & z \geq L \end{cases} \quad (6)$$

where $k_0(\omega) = \omega/c$ is the vacuum wave number, $k(\omega) = \omega \mathcal{N}(\omega)/c$ is the complex wavenumber in the medium, and the complex index of refraction $\mathcal{N}(\omega)$ is defined by

$$\mathcal{N}(\omega) = \sqrt{1 + \chi(\omega)} = \sqrt{\varepsilon(\omega)} = n(\omega) + i\kappa(\omega). \quad (7)$$

In Eq. (7) we must take the branch of the square root so that $n(\omega)$ and $\kappa(\omega)$ are positive for all ω in the right half of the upper half plane. In Eq. (6), $\hat{E}_i(\omega)$ and $\hat{E}_r(\omega)$ describe the incident and reflected fields at $z = 0$ on the vacuum side of the interface, $\hat{E}_f(\omega)$ and $\hat{E}_b(\omega)$ describe the forward and backward traveling fields at $z = 0$ on the medium side of the interface, and $\hat{E}_t(\omega)$ gives the transmitted field in vacuum at $z = L$.

Using this formalism, we can model an arbitrary one-dimensional incident pulse originating at $z = -\infty$. The incident pulse is specified by choosing $\hat{E}_i(\omega)$, and the remaining fields in Eq. (6) are then determined by requiring that $\hat{E}(z, \omega)$ and $\hat{E}'(z, \omega)$ be continuous across the boundaries at $z = 0$ and $z = L$. This process produces the following Fresnel-type relationships for the fields in Eq. (6):

$$\begin{aligned} \hat{E}_t(\omega) &= t(\omega) \hat{E}_i(\omega) \\ \hat{E}_r(\omega) &= r(\omega) \hat{E}_i(\omega) \\ \hat{E}_f(\omega) &= f(\omega) \hat{E}_i(\omega) e^{-ik(\omega)L} \\ \hat{E}_b(\omega) &= b(\omega) \hat{E}_i(\omega) e^{ik(\omega)L} \end{aligned} \quad (8)$$

where

$$\begin{aligned} t(\omega) &= \frac{4\mathcal{N}(\omega)}{(1 + \mathcal{N}(\omega))^2 e^{-ik(\omega)L} - (1 - \mathcal{N}(\omega))^2 e^{ik(\omega)L}} \\ r(\omega) &= 2i \frac{\sin(k(\omega)L)}{\frac{\mathcal{N}(\omega)+1}{\mathcal{N}(\omega)-1} e^{-ik(\omega)L} - \frac{\mathcal{N}(\omega)-1}{\mathcal{N}(\omega)+1} e^{ik(\omega)L}} \\ f(\omega) &= \frac{2(\mathcal{N}(\omega) + 1)}{(1 + \mathcal{N}(\omega))^2 e^{-ik(\omega)L} - (1 - \mathcal{N}(\omega))^2 e^{ik(\omega)L}} \\ b(\omega) &= \frac{2(\mathcal{N}(\omega) - 1)}{(1 + \mathcal{N}(\omega))^2 e^{-ik(\omega)L} - (1 - \mathcal{N}(\omega))^2 e^{ik(\omega)L}} \end{aligned} \quad (9)$$

Each of the electric fields in Eq. (8) has an associated magnetic field specified by Eq. (4).

Energy exchange is well-described in the context of Poynting's theorem,

$$\dot{u}(z, t) + c\nabla \cdot \mathbf{S}(z, t) = 0, \quad (10)$$

which connects the energy density $u(z, t)$ with the Poynting flux $\mathbf{S}(z, t) = \mathbf{E}(z, t) \times \mathbf{H}(z, t)$ at each point z in the medium. We use the Heaviside-Lorentz system of units with $\epsilon_0 = 1 = \mu_0$, and indicate the partial time derivative with a dot (as in \dot{u}). The energy density is typically divided as

$$u(z, t) = u_{\text{field}}(z, t) + u_{\text{int}}(z, t) \quad (11)$$

where the field energy density is given by

$$u_{\text{field}}(z, t) = \frac{1}{2} \mathbf{H}(z, t) \cdot \mathbf{H}(z, t) + \frac{1}{2} \mathbf{E}(z, t) \cdot \mathbf{E}(z, t) \quad (12)$$

and the energy density associated with pulse-medium interactions is given by

$$u_{\text{int}}(z, t) = \int_{-\infty}^t d\tau \mathbf{E}(z, \tau) \cdot \dot{\mathbf{P}}(z, \tau). \quad (13)$$

The total “planer” energy for this system is given by

$$U_{\text{tot}} := \int_{-\infty}^{+\infty} dz u(z, t). \quad (14)$$

U_{tot} is conserved (i.e. independent of t), and will be finite for incident fields with finite duration. We can spatially divide energy integral Eq. (14) as

$$U_{\text{tot}} = U_{(-\infty, 0]}(t) + U_{[0, L]}(t) + U_{[L, \infty)}(t) \quad (15)$$

where $U_{(-\infty, 0]}(t)$, $U_{[0, L]}(t)$, and $U_{[L, \infty)}(t)$ are, respectively, the total energy densities to the left of the medium, inside the medium, and to the right of the medium at a given time t . Before the pulse arrives at the first interface, U_{tot} is given by the incident energy field energy $U_{(-\infty, 0]}(-\infty)$. After all exchange processes have ceased, the energy is split between reflected energy $U_{(-\infty, 0]}(\infty)$, dissipated thermal energy $U_{[0, L]}(\infty)$, and transmitted energy $U_{[L, \infty)}(\infty)$. During the interaction, the energy in the medium is divided as in the point-wise case between field energy and energy stored in the medium

$$U_{[0, L]}(t) = U_{[0, L], \text{field}}(t) + U_{\text{int}}(t) \quad (16)$$

To define a meaningful notion of real-time loss at an arbitrary time t , we divide the incident field into the past field prior to t and the future field subsequent to t . The past field is fixed for any given time t , but conceptually we can consider various future fields that would change eventual dissipation in the medium. We can then find the future field that results in the minimum eventual loss. (We make the process for finding this field mathematically precise in the next section.) With this optimum future field in hand, we can then divide the energy in the medium as

$$U_{\text{int}}(t) = U_{\text{irrec}}(t) + U_{\text{rec}}(t), \quad (17)$$

where $U_{\text{irrec}}(t)$ is energy stored in the medium that must eventually be dissipated, and $U_{\text{rec}}(t)$ is the energy stored in the medium that could potentially be returned to the field through either reflection or transmission with an appropriate future field. Analogous to u_{irrec} in the point-wise case, $U_{\text{irrec}}(t)$ gives an upper bound for valid notions of loss in an extended medium.

The above approach for calculating $U_{\text{irrec}}(t)$ treats both the reflected and transmitted field energy as being equally well “recovered” from the medium. In propagation systems, one often focuses on the energy that is transmitted in the positive z direction, so that both dissipated and

reflected energy are equally regarded as “lost.” For this sort of system it is more natural to divide the energy stored in the medium as

$$U_{\text{int}}(t) = U_{\text{loss}}(t) + U_{\text{trans}}(t), \quad (18)$$

where $U_{\text{loss}}(t)$ represents the energy in the medium that must eventually be lost due either to dissipation or reflection, and $U_{\text{trans}}(t)$ represents the energy in the medium that could be eventually transmitted from the medium in the positive z direction. In Section 3 we illustrate how to derive a formula for $U_{\text{loss}}(t)$. Calculating $U_{\text{irrec}}(t)$ can be handled as a special case of this more general definition.

3. Minimizing future loss

The total eventual loss in our system is given by:

$$U_{\text{loss}}(\infty) = c \int_{-\infty}^{+\infty} d\omega |\hat{E}_r(0, \omega)|^2 + \int_{-\infty}^{+\infty} d\omega \int_0^L dz \rho(\omega) |\hat{E}(z, \omega)|^2 \quad (19)$$

where $\rho(\omega) = \text{Re}[-i\omega\chi(\omega)]$. The first term in Eq. (19) gives the eventual loss due to reflection $U_{(-\infty, 0]}(\infty)$, and the second term gives the eventual loss due to dissipation $U_{[0, L]}(\infty)$. We seek to find the minimum possible $U_{\text{loss}}(\infty)$ while treating the past incident field (before time t) as fixed and allowing the future field to vary. Utilizing Eq. (2), Eq. (6), Eq. (8), and Eq. (9), we can manipulate Eq. (19) into the form

$$U_{\text{loss}}(\infty) = L \frac{\gamma}{\omega_p^2} \int_{-\infty}^{\infty} d\omega m(\omega) |\omega\chi(\omega)\hat{E}_i(0, \omega)|^2 \quad (20)$$

where

$$m(\omega) = \frac{\omega_p^2}{\gamma(L/c)} \frac{M(\omega)}{|-i\omega\chi(\omega)|^2}, \quad (21)$$

and

$$M(\omega) = |r(\omega)|^2 + \rho(\omega) \int_0^{L/c} d\tau \left| f(\omega)e^{-i\omega\mathcal{N}(\omega)\tau} + b(\omega)e^{i\omega\mathcal{N}(\omega)\tau} \right|^2. \quad (22)$$

The parameter γ describes the dissipation rate at high frequency, and is given by

$$\gamma = \lim_{\omega \rightarrow \infty} - \frac{\omega \text{Im} \chi(\omega)}{\text{Re} \chi(\omega)}, \quad (23)$$

and the plasma frequency ω_p is given by

$$\omega_p^2 = \lim_{\omega \rightarrow \infty} -\omega^2 \chi(\omega). \quad (24)$$

When computing $m(\omega)$, it is useful to note there that the integral in Eq. (22) can be calculated as

$$\begin{aligned} & \int_0^{\tau_L := L/c} d\tau \left| f(\omega)e^{-i\omega\mathcal{N}(\omega)\tau} + b(\omega)e^{+i\omega\mathcal{N}(\omega)\tau} \right|^2 \\ &= \left(|f(\omega)|^2 e^{\tau_L \omega \kappa(\omega)} + |b(\omega)|^2 e^{-\tau_L \omega \kappa(\omega)} \right) \frac{\sinh(\tau_L \omega \kappa(\omega))}{\omega \kappa(\omega)} \\ &+ \left(f(\omega)b^*(\omega)e^{-i\tau_L \omega n(\omega)} + b(\omega)f^*(\omega)e^{+i\tau_L \omega n(\omega)} \right) \frac{\sin(\tau_L \omega n(\omega))}{\omega n(\omega)}. \quad (25) \end{aligned}$$

The quantity $m(\omega)$ in Eq. (21) is real for real frequencies ω and its complex conjugate m^* satisfies $m^*(\omega) = m(-\omega^*)$, so that m is the Fourier transform of a real, even function. The form of $m(\omega)$ was chosen in Eq. (21) such that we have $\lim_{\omega \rightarrow \infty} m(\omega) = 1$, and also so that the limit as $\omega \rightarrow 0$ gives

$$\lim_{\omega \rightarrow 0} m(\omega) = \frac{\omega_p^2}{\gamma(L/c)} \left(\frac{(L/c)^2}{4} + \frac{\text{Im}[\chi'(0)]}{\chi^2(0)} (L/c) \right), \quad (26)$$

so that Eq. (28) is well-behaved near $\omega = 0$. It is thus possible to factor m as

$$m(\omega) = m_+(\omega)m_+(-\omega) \quad (27)$$

where $m_+(\omega)$ and its reciprocal $1/m_+(\omega)$ are analytic and tending to unity in the upper half ω plane, and $m_+^*(\omega) = m_+(-\omega^*)$. The factorization Eq. (27) is accomplished according to

$$m_+(\omega) = (\exp \circ F \circ \theta_0^+ \circ F^{-1} \circ \log) m(\omega) \quad (28)$$

where θ_0^+ is the unit step function supported for positive times and \circ is the composition operator. (I.e., to calculate the right hand side of Eq. (28) one computes the exponential of the Fourier transform of the step function multiplied by the inverse Fourier transform of the log of $m(\omega)$.) The logarithm in Eq. (28) goes to zero for large ω as $1/\omega^2$, so that the inverse Fourier transform F^{-1} results in a continuous function of time.

Using the factorization of $m(\omega)$ in Eq. (27), and introducing the definition $\hat{P}_{\text{eff}}(\omega) \equiv -i\omega m_+(\omega)\chi(\omega)\hat{E}_i(0, \omega)$ we can recast Eq. (20) as

$$U_{\text{loss}}(\infty) = L \frac{\gamma}{\omega_p^2} \int_{-\infty}^{+\infty} d\omega \left| \hat{P}_{\text{eff}}(\omega) \right|^2. \quad (29)$$

Then via Parseval's theorem, we have

$$U_{\text{loss}}(\infty) = L \frac{\gamma}{\omega_p^2} \int_{-\infty}^{+\infty} d\tau \dot{P}_{\text{eff}}^2(\tau), \quad (30)$$

where we have dropped the absolute value operation because the time-domain transform

$$\dot{P}_{\text{eff}}(\tau) := F^{-1} \left[\hat{P}_{\text{eff}}(\omega) \right] \quad (31)$$

is real-valued due to the symmetry of $\hat{P}_{\text{eff}}(\omega)$. The quantity P_{eff} has units of polarization, although it is not associated with any particular point in the slab, but rather with the slab in its entirety. Because $m_+(\omega)$ is analytic in the upper half ω plane, $P_{\text{eff}}(\tau)$ depends only on past values of the incident field $E_i(\tau)$. Equivalently, with linearity and stationarity (no absolute origin in time), if $E_i(0, \tau < t) = 0$ then we must have $P_{\text{eff}}(\tau < t) = 0$. Conversely, because $1/m_+(\omega)$ is also analytic in the upper half plane, if $P_{\text{eff}}(\tau < t) = 0$ then we must have $E_i(0, \tau < t) = 0$. This “reciprocal causality” property will be important in assuring that our notion of loss is unique and well-defined.

To distinguish past and future losses, we write the incident field in terms of its past and future components

$$(E_i)_t^-(\tau) = \begin{cases} E_i(\tau), & \tau \leq t \\ 0, & \tau > t \end{cases}, \quad (32)$$

$$(E_i)_t^+(\tau) := \begin{cases} 0, & \tau \leq t \\ E_i(\tau), & \tau > t \end{cases}.$$

The fields in Eq. (32) are evaluated at $z = 0$, but we have omitted the spatial coordinate to reduce notational clutter. Then, we write $P_{\text{eff}}(\tau)$ as $P_{\text{eff}}[E_i](\tau)$ to explicitly show its dependence on the incident field E_i , and then use Eq. (32) to write Eq. (30) to explicitly show the dependence on past and future fields as

$$U_{\text{loss}}[E_i](\infty) = L \frac{\gamma}{\omega_p^2} \int_{-\infty}^t d\tau \dot{P}_{\text{eff}}^2 [(E_i)_t^- + (E_i)_t^+] (\tau) + L \frac{\gamma}{\omega_p^2} \int_t^{+\infty} d\tau \dot{P}_{\text{eff}}^2 [(E_i)_t^- + (E_i)_t^+] (\tau). \quad (33)$$

Because $\dot{P}_{\text{eff}}^2(\tau)$ depends only on past values of the field, we can then recast the first term and write

$$U_{\text{loss}}[E_i](\infty) = L \frac{\gamma}{\omega_p^2} \int_{-\infty}^t d\tau \dot{P}_{\text{eff}}^2 [(E_i)_t^-] (\tau) + L \frac{\gamma}{\omega_p^2} \int_t^{+\infty} d\tau \dot{P}_{\text{eff}}^2 [(E_i)_t^- + (E_i)_t^+] (\tau). \quad (34)$$

Because $\dot{P}_{\text{eff}}(\tau)$ is real, the first term in Eq. (34) is monotonic increasing. The second term must also be nonnegative, so to minimize $U_{\text{loss}}(\infty)$ given a fixed past field, we seek an ‘‘optimum’’ future field $(E_i)_{t,\text{opt}}^+$ such that the second part of Eq. (34) vanishes:

$$L \frac{\gamma}{\omega_p^2} \int_t^{+\infty} d\tau \left| \dot{P}_{\text{eff}} [(E_i)_t^- + (E_i)_{t,\text{opt}}^+] (\tau) \right|^2 \equiv 0, \quad \tau > t. \quad (35)$$

Since the integrand in Eq. (35) is nonnegative, it is necessary to demand

$$\dot{P}_{\text{eff}} [(E_i)_t^- + (E_i)_{t,\text{opt}}^+] (\tau) \equiv 0, \quad (\tau > t). \quad (36)$$

After some transforms and algebra, we can solve Eq. (36) to find the optimum future field

$$(E_i)_{t,\text{opt}}^+ = - (F^{-1} \circ e^{i\omega t} \circ M_+^{-1} \circ F \circ \theta_0^+ \circ F^{-1} \circ M^+ \circ e^{-i\omega t} \circ F) (E_i)_t^-, \quad (37)$$

where

$$M_+(\omega) := -i\omega m_+(\omega) \chi(\omega). \quad (38)$$

Importantly

$$M_+^{-1}(\omega) := \frac{1}{M_+(\omega)} = \frac{1}{-i\omega m_+(\omega) \chi(\omega)} \quad (39)$$

is analytic in the (open) upper half plane, so that the last steps in Eq. (37) do in fact render $(E_i)_{t,\text{opt}}^+$ as a time series supported only after $\tau = t$.

With the optimum future field, Eq. (34) now gives an unambiguous meaning to our concept of loss. The fixed past losses at any time t are given by

$$U_{\text{loss}}(t) = L \frac{\gamma}{\omega_p^2} \int_{-\infty}^t d\tau \dot{P}_{\text{eff}}^2 [(E_i)_t^-] (\tau). \quad (40)$$

Future losses, given by the second term in Eq. (34), can in principle be avoided by replacing the future field with its optimum value, calculated using Eq. (37).

As indicated in the previous section, it is possible to use this same derivation to arrive at a formula for $U_{\text{irrec}}(t)$, which treats both reflection and transmission as equally valid methods of recovering energy stored in the medium back to the field. The formula for $U_{\text{irrec}}(t)$ has the same form as Eq. (40), except that in Eq. (22) the definition of $M(\omega)$ is replaced by

$$M_{\text{irrec}}(\omega) = \rho(\omega) \int_0^{L/c} d\tau \left| f(\omega) e^{-i\omega \mathcal{N}(\omega)\tau} + b(\omega) e^{i\omega \mathcal{N}(\omega)\tau} \right|^2, \quad (41)$$

i.e., the reflection term is set to zero.

4. Examples

To illustrate the use of the concepts, consider the specific case of a Lorentz oscillator medium where $\chi(\omega)$ has the form

$$\chi(\omega) = \sum_{j=1}^N \chi_j(\omega) = \sum_{j=1}^N \frac{f_j \omega_{p_j}^2}{\omega_j^2 - i\gamma_j \omega - \omega^2}. \quad (42)$$

The parameters f_j , ω_{p_j} , ω_j , and γ_j are the oscillator strength, plasma frequency, resonant frequency, and damping rate of the j^{th} Lorentz oscillator. We consider a Gaussian pulse of the form

$$E_i(t) = E_0 e^{-t^2/\tau^2} \cos(\bar{\omega}t + \phi) \quad (43)$$

incident on this medium and study the energy dynamics in this interaction.

For our first example, consider a double resonance medium with parameters

$$\begin{aligned} \gamma_1 &= 0.1\gamma_2 \\ \omega_1 &= \omega_2 = 100\gamma_2 \\ f_1 \omega_{p_1}^2 &= -9.95\gamma_2^2 \\ f_2 \omega_{p_2}^2 &= 100\gamma_2^2 \\ L &= c/\gamma_2 \end{aligned} \quad (44)$$

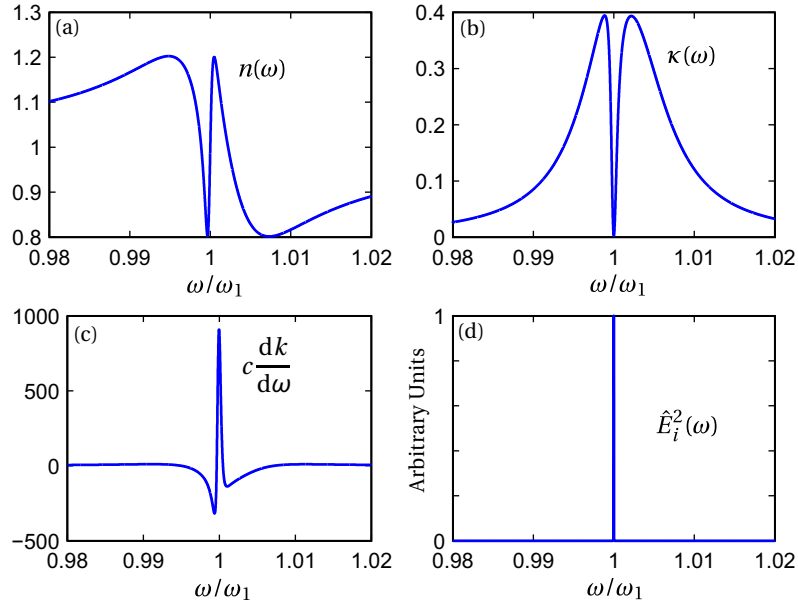


Fig. 1. The real (a) and imaginary (b) parts of the the index of refraction for the parameters in Eq. (44). (c) The group delay function for this medium. (d) The power spectrum of the pulse, which has been arbitrarily normalized to have a maximum value of one. This pulse-medium combination should exhibit moderately slow propagation delays, around 900 times slower than c .

For our incident field, we choose a relatively narrowband pulse with

$$\begin{aligned}\tau &= 1000\gamma_2^{-1} \\ \bar{\omega} &= 100\gamma_2 \\ \phi &= 0.\end{aligned}\tag{45}$$

Figures 1(a)–1(c) plot $n(\omega)$, $\kappa(\omega)$, and $dk/d\omega$ (the group delay function) for this medium. Note that the pulse spectrum is centered in a mostly transparent region where index varies rapidly, resulting in a group delay function that predicts moderately slow delay times about 900 times slower than c . We calculated the spatial distribution of the energy densities associated with this pulse, and Fig. 2 shows an animation of the evolution of the distribution as time progresses. Figure 2(a) shows the large scale behavior of this pulse as it moves from the vacuum on the left, through the medium (indicated by the vertical green line), and then into the vacuum on the right. The blue solid line indicates the distribution of field energy, while a dotted red line indicates how the pulse would have propagated if the medium were not there for comparison. In both cases we have time-averaged the rapid fluctuations at the optical frequency to give us the smooth envelope of the distributions. As expected, the pulse propagates slowly through the medium and emerges during the trailing edge of the dotted reference pulse.

Figure 2(b) plots $u_{\text{field}}(z, t)$ and Fig. 2(c) plots $u_{\text{int}}(z, t)$ in the medium. The field energy in the medium is the portion of the energy that is actively being transported, and shows a peak traversing the medium approximately 900 times slower than c . The total energy in the medium

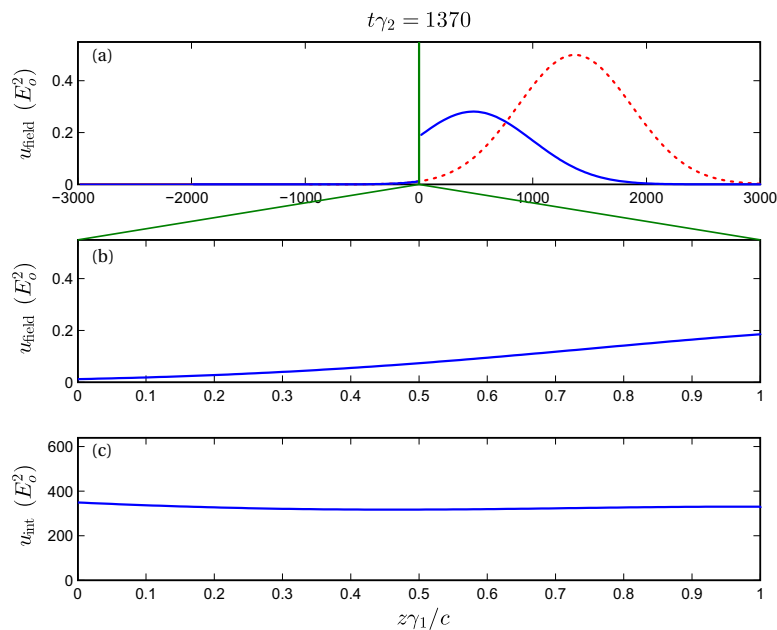


Fig. 2. An animation of the spatial distribution of energy densities as the pulse defined in Eq. (45) traverses the medium defined in Eq. (44) (Media 1). (a) The propagation in vacuum before and after the medium, represented by the vertical line at $z = 0$. The solid line plots the field energy distribution with the medium present and the dotted line plots the field energy distribution would have been if the medium were not present for comparison. (b) The distribution of u_{field} in the medium. (c) The distribution of u_{int} in the medium. All plots have been locally time-averaged to remove the rapid fluctuations at the carrier frequency.

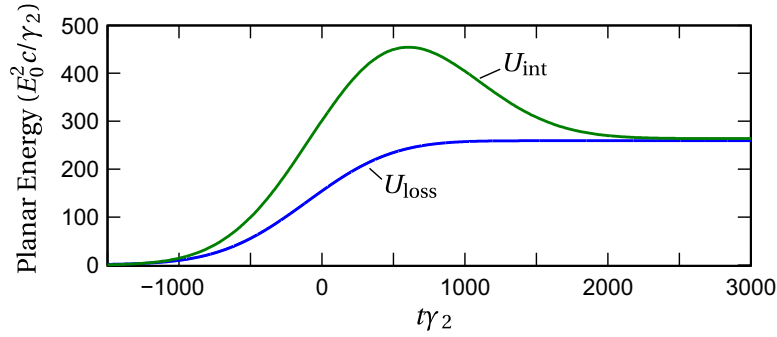


Fig. 3. The total energy stored in the medium U_{int} compared with the real-time loss U_{loss} of energy for the pulse-medium combination illustrated in Fig. 2.

$U_{\text{int}}(t)$ is stationary, and can be divided into a portion U_{trans} that could be transmitted with the appropriate future pulse, and a portion U_{loss} that must remain in the medium.

Figure 3 plots the total energy stored in the medium $U_{\text{int}}(t)$ compared with the real-time loss $U_{\text{loss}}(t)$ calculated using Eq. (40). U_{trans} is the difference of these two curves. Comparing U_{field} to U_{trans} , we find that only about 0.2% of the undissipated energy is actually moving via Poynting flux at any given time while the rest remains stationary in the medium. Thus, the average speed of all the energy is heavily influenced by the stationary portion of the energy and the dramatic slow propagation is observed.

Notice that a large fraction of the incident energy is lost from this Gaussian pulse during the times when it is entering the medium. Eventually, the remaining energy is transmitted into the vacuum to the right, and U_{int} and U_{loss} take on the same value at large times (i.e. all the energy remaining in the medium has been dissipated). We can engineer a more efficient extraction of energy by using Eq. (37) to calculate a second half of a pulse that will extract all energy available in the medium after a certain time. We take the pulse before $t = 0$ to be as defined by Eq. (45), and after $t = 0$ we append the optimum recovery pulse calculated by Eq. (37). Figure 4(a) shows the temporal profile of the original incident pulse, and Fig. 4(b) shows the pulse with the optimum recovery field appended to the second half.

Figure 5 shows an animation of the pulse in Fig. 4(b) propagating through the medium defined by Eq. (44). The optimum field contains a delta function represented by the arrow in Fig. 4(b). This feature is not resolved in the animation because it is much too narrow for the

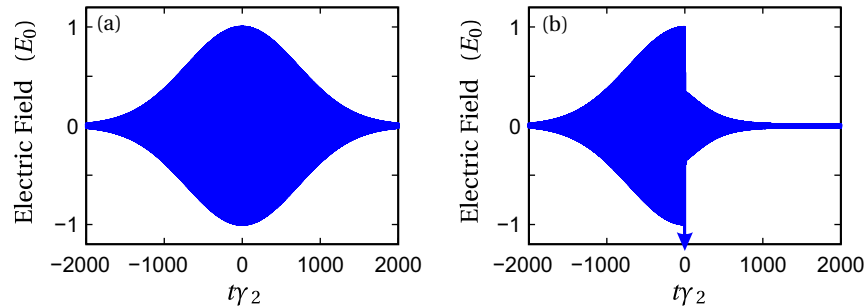


Fig. 4. (a) The temporal profile of a the Gaussian pulse Eq. (43) with the parameters in Eq. (45). (b) The first half of the pulse is the same as (a), but the second half is the optimum future recovery field for the medium described in Eq. (44).

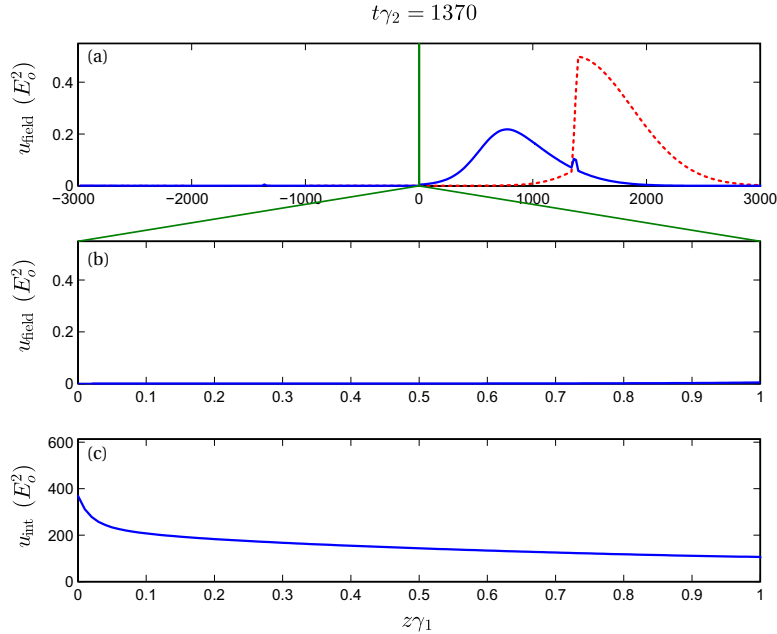


Fig. 5. An animation of the spatial distribution of energy densities as the pulse defined in Eq. (45) traverses the medium defined in Eq. (44) (Media 2). (a) The propagation in vacuum before and after the medium, represented by the vertical line at $z = 0$. The solid line plots the field energy distribution with the medium present and the dotted line plots the field energy distribution would have been if the medium were not present for comparison. (b) The distribution of u_{field} in the medium. (c) The distribution of u_{int} in the medium. All plots have been locally time-averaged to remove the rapid fluctuations at the carrier frequency.

resolution of the movie, but is included in the calculations used to generate the movie. A true delta function would not be possible to create in a physical experiment. Nevertheless, in our simulation a narrow downward peak in the pulse profile is sufficient to capture the essential behavior of the recovery field.

For the example parameters we have chosen, there is very little reflected light because the index of refraction for the medium is near unity for the frequencies in the pulse. In cases where there is significant reflection, the recovery field can contain repeated pulses separated by the round-trip traversal time of the medium. This sequence of pulses results from our requirement that the optimal recovery pulse cause the maximum amount of light to be transmitted, rather than just removed from the medium. The sequence of afterpulses interferes with the backward traveling portion of the field in the medium so as to cause the energy to be transmitted to the right rather than reflected to the left. If one wishes to avoid this feature in a recovery pulse, it is necessary use Eq. (41) in calculating the recovery field as discussed previously.

In Fig. 6 we plot the real-time loss U_{loss} and the total energy in the medium U_{int} for this modified pulse. For comparison, the plots from Fig. 3 (for the unmodified pulse in Fig. 4(a)) are repeated as dashed lines. Note that after $t = 0$, when we switch to the optimal recovery field, there is no additional loss for this pulse. The energy that has been deposited in the medium prior to $t = 0$ is extracted by the optimum recovery field and produces the delayed portion of energy transmitted to the vacuum after the medium.

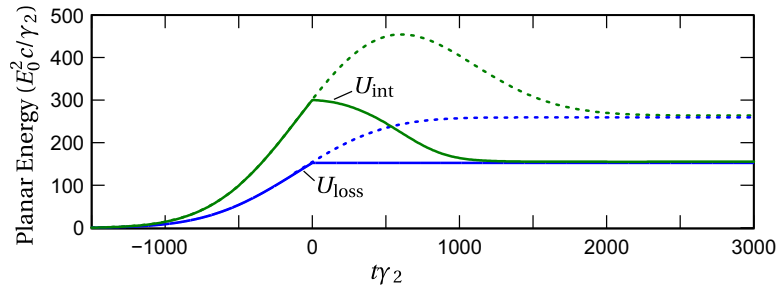


Fig. 6. The solid lines plot the total energy stored in the medium U_{int} and the real-time loss U_{loss} of energy for the pulse-medium combination illustrated in Fig. 5. Dashed lines plot the same quantities from Fig. 3 for comparison.

5. Conclusion

We have introduced a method for calculating the real-time loss of energy stored in a medium that is valid for pulses propagating in extended media. This method for calculating dissipation is consistent with Maxwell's equations and allows one to analyze real-time loss in propagation settings. A complete understanding of real-time loss is important in applications such as slow and fast pulse propagation experiments where the timing of energy flows in and out of the pulse are crucial. We have illustrated the use of this formalism in analyzing a typical "slow light" propagation situation, and illustrated a simple method for engineering pulse shapes for optimal energy recovery. While this example employed a specific model (the Lorentz model), the formalism is independent of the model used to represent the material.